

Strategies for High-Performance Solid-State Triplet-Triplet Annihilation Based Photon Upconversion

*Ting-An Lin, Collin F. Perkinson, and Marc A. Baldo**

T.-A. Lin, Prof. M. A. Baldo

Department of Electrical Engineering and Computer Science, Massachusetts Institute of Technology,
77 Massachusetts Avenue, Cambridge, Massachusetts, 02139, United States

E-mail: baldo@mit.edu

C. F. Perkinson

Department of Chemistry, Massachusetts Institute of Technology, 77 Massachusetts Avenue,
Cambridge, Massachusetts, 02139, United States

Keywords: solid-state photon upconversion, triplet-triplet annihilation, triplet-charge annihilation

Abstract

Photon upconversion via triplet-triplet annihilation (TTA) has achieved high efficiencies in solution and within polymer matrices that support molecular migration systems. It has diverse potential applications including bioimaging, optical sensors, and photovoltaics. To date, however, the reported performance of TTA in rigid solid-state systems is substantially inferior, which may complicate the integration of TTA in other solid-state devices. Here, solid-state loss mechanisms in a green-to-blue upconversion system are investigated, and three specific losses are identified: energy back transfer, sensitizer aggregation, and triplet-charge annihilation (TCA). Strategies are demonstrated to mitigate energy back transfer and sensitizer aggregation, and a completely dry-processed solid-state TTA upconversion system having an upconversion efficiency of $\sim 2.5\%$ (by the convention of maximum efficiency being 100%) at a relatively low excitation intensity of 238 mW/cm^2 is reported. This device is the first demonstration of dry-processed solid-state TTA comparable to solution-processed solid-state systems. The strategies reported here can be generalized to other upconversion systems and offer a route to achieving higher performance solid-state TTA upconversion devices that are compatible with applications sensitive to solvent damage.

This is the author manuscript accepted for publication and has undergone full peer review but has not been through the copyediting, typesetting, pagination and proofreading process, which may lead to differences between this version and the [Version of Record](#). Please cite this article as [doi: 10.1002/adma.201908175](#).

This article is protected by copyright. All rights reserved.

Among the techniques capable of converting multiple low-energy photons into a higher-energy photon, triplet-triplet annihilation (TTA) is promising for a variety of applications because a low-intensity incoherent light source is sufficient to initiate the upconversion process.^[1–3] A TTA system typically consists of two main components: (1) a triplet sensitizer that absorbs the excitation light, generates singlet excitons, and then creates triplet excitons through efficient intersystem crossing (transition from the spin-singlet state to the spin-triplet state); and (2) an annihilator that combines multiple triplet excitons into a higher-energy singlet exciton.^[3–6] Studies of TTA upconversion systems in solutions or polymers that support molecular migration (quasi-solids) have successfully achieved upconversion efficiencies beyond 30%.^[7–10] At the same time, the threshold intensities at which these devices reach their peak efficiencies are low (less than one sun, or $<100 \text{ mW/cm}^2$), demonstrating their potential for applications such as photoredox catalysis and drug release control.^[11,12]

Despite the relative success of solution- and quasi-solid-based TTA upconversion systems, some applications that would benefit from photon upconversion necessitate rigid, solvent-free solid-state systems. Unfortunately, the peak efficiencies reported to-date for solid-state upconversion systems are substantially lower than those reported for solution- and quasi-solid-based systems.^[13,14] This discrepancy is largely a result of three factors: (1) The low triplet exciton mobility in the sensitizer limits the triplet transfer efficiency to the annihilator, (2) annihilator-to-sensitizer exciton back transfer competes with radiative emission of the upconverted excitons, and (3) molecular aggregation of the sensitizer results in nonradiative triplet recombination before triplet transfer to the annihilator can be realized (**Figure 1**).^[13,14] Studies on polymer-based solid-state upconversion systems have adopted the architecture of doping the sensitizer into the annihilator matrix to ensure efficient triplet transfer.^[13] In addition, introducing an emissive dye to the annihilator has been

shown to be beneficial for efficient upconverted emission. This technique is capable of reducing concentration quenching of the annihilator by trapping the singlet excitons in the annihilator,^[15] as well as alleviating back-transfer losses if the emissive dye is physically separated from the sensitizer.^[14] Here, we rigorously examine these dynamics using vacuum-deposited thin films that are compatible with applications such as photovoltaics and organic light emitting diodes.^[16–18]

The loss mechanisms in solid-state TTA upconversion are investigated within a well-studied green-to-blue upconversion material system: platinum(II)octaethylporphyrine (PtOEP) as sensitizer and an anthracene derivative as annihilator.^[9,14,19,20] The annihilator is selected from previous studies on TTA-based blue organic light emitting diodes because the material properties in evaporated films are known. We found the well-known TTA host, 2-methyl-9,10-bis(naphthalene-2-yl)anthracene (MADN), a suitable candidate as the annihilator due to its energy alignment with the sensitizer, PtOEP.^[21,22] Furthermore, doping the annihilator with 3 vol.% of the emitter molecule 4,4'-bis[4-(diphenylamino)styryl]biphenyl (BDAVB) improves the photoluminescence quantum yield (PLQY) by a factor of two by trapping the singlet excitons from MADN to reduce concentration quenching.^[21]

Four upconversion device structures are compared in this work. First, we fabricate a simple bilayer of PtOEP (2 nm)/MADN: 3 vol.% BDAVB (50 nm), which we call the “Bilayer” device. This structure has been used in thermal evaporation-based TTA upconversion devices and has been shown to exhibit upconversion.^[15,23] Though easy to fabricate, back transfer is inevitable in a bilayer device architecture owing to the proximity of the annihilator and the sensitizer. Indeed, back transfer can be expected in our system based on the overlap between the absorption spectrum of PtOEP and the photoluminescence (PL) spectrum of MADN:BDAVB (**Figure 2a**). Therefore, we insert 1-[2,5-dimethyl-4-(1-pyrenyl)phenyl]pyrene (DMPPP), which has higher singlet energy than MADN and BDAVB, between PtOEP and MADN:BDAVB to reduce direct Förster resonance energy transfer (FRET) from the annihilator to the sensitizer.^[24] To ensure that DMPPP does not block triplet transfer

from PtOEP to MADN, phosphorescence spectra of DMPPP and MADN are measured to confirm the alignment of their triplet levels (**Figure S1**). Although phosphorescence spectra suggest that the triplet energy of DMPPP might be slightly above that of PtOEP, triplet transfer from PtOEP to DMPPP is confirmed through observation of upconverted PL from DMPPP in a bilayer of PtOEP/DMPPP (**Figure S2**).^[25] This second device, with the structure PtOEP (2 nm)/DMPPP (5 nm)/MADN: 3 vol.% BDAVBi (50 nm), we hereafter call the “Buffer” device (**Figure 2b–c**).

In addition to back transfer, PtOEP is known to form excimer and aggregate states in neat films,^[26] which can trap triplet excitons prior to transferring to MADN. As shown in **Figure 2a**, the absorption spectrum of PtOEP in neat film is distorted in the range of ~530–570 nm compared to its absorption spectrum in solution,^[27] indicating a new state caused by molecular aggregation. The device architecture of blending the sensitizer into the annihilator at a low concentration, widely adopted in polymer studies,^[13] is applied to suppress aggregation of PtOEP and ensure effective triplet exciton transfer to MADN. This results in a single film of MADN: 0.4 vol.% PtOEP: 3 vol.% BDAVBi (100 nm) as our third device, hereafter called the “Triple-doped” device. However, back transfer in the Triple-doped device is expected to be worse than in the Bilayer device due to the shorter average separation between MADN and PtOEP molecules. As such, we test a fourth device based on a modification of the Bilayer device by doping PtOEP into DMPPP at 40 vol.% to suppress aggregation. The absorption spectrum of this modified sensitizer resembles that of the absorption spectrum of PtOEP in solution,^[27] confirming that molecular aggregation is effectively suppressed (**Figure 2a**). The structure of this device, which we call the “DMPPP-doped” device, is DMPPP: 40 vol.% PtOEP (5 nm)/MADN: 3 vol.% BDAVBi (50 nm). **Figure 2d** summarizes the device structures and the design concept for the four upconversion devices studied in this work.

To compare the performance of the four upconversion devices, we first characterize their upconversion efficiencies. Based on **Figure 1**, the external quantum efficiency (EQE) of the devices can be written as

$$EQE = Abs \times \phi_{DET} \times \frac{\phi_{TTA}}{2} \times (1 - \phi_{BT}) \times \phi_{PL}, \quad (1)$$

where Abs is the absorption of the device at 532 nm excitation, ϕ_{DET} is the efficiency of triplet transfer from PtOEP to MADN, ϕ_{TTA} is the TTA efficiency for MADN, and ϕ_{BT} is the back-transfer efficiency. ϕ_{PL} is the PLQY of MADN:BDAVBi at 405 nm excitation, which is determined to be $(90 \pm 0.55)\%$ using the integrating sphere measurement technique proposed by de Mello et al.^[28] ϕ_{TTA} is divided by two in order to follow the convention of maximum ϕ_{TTA} being 100%, giving a maximum EQE of 50% because TTA is a two-to-one photon conversion process. The upconversion efficiency (ϕ_{UC}) is defined as the ratio of the number of upconverted photons emitted to the number of low-energy photons absorbed,^[3,6] giving

$$\phi_{UC} = 2 \times EQE / Abs, \quad (2)$$

from Equation (1), with the factor of 2 scaling the maximum ϕ_{UC} to 100%.

We measure the EQE for all of the devices and the Abs of the Bilayer, Buffer, and DMPPP-doped devices with the same technique as used when measuring the PLQY of MADN:BDAVBi. The absorption of the Triple-doped device is beyond the resolution of our integrating sphere measurement. Therefore, the absorption is instead determined by linear extrapolation from the other three devices (Supporting Information). ϕ_{UC} can then be calculated by Equation (2), giving an upconversion efficiency of $(0.34 \pm 0.06)\%$, $(0.47 \pm 0.08)\%$, $(2.05 \pm 0.12)\%$, and $(2.46 \pm 0.12)\%$ for the Bilayer, Buffer, Triple-doped, and DMPPP-doped devices, respectively.

To understand the underlying physical reasons for the differences in ϕ_{UC} between the devices, we measure the PL decay dynamics of MADN:BDAVBi in the upconversion devices and in an

MADN:BDAVBi-only film with 372 nm excitation. At this excitation wavelength, the singlet excitons in MADN:BDAVBi are excited directly, and the quenching of the PL in the upconversion devices originates from back transfer. As shown in **Figure 3a**, only the fast decay component of MADN:BDAVBi is quenched when the sensitizer is present. The back-transfer efficiency is therefore determined to be $\phi_{BT} = 1 - \tau/\tau_0$, where τ_0 is the intrinsic lifetime for MADN:BDAVBi (1.007 ns), and τ denotes the lifetime for the upconversion devices (**Figure 3b**). We find the back-transfer efficiency ϕ_{BT} to be 7.9%, 5.5%, 60.3%, and 7.5% for the Bilayer, Buffer, Triple-doped, and DMPPP-doped devices, respectively (see Supporting Information, **Figure S3**, and **Figure S4a–b** for details).

The ideal implementation of TTA-based upconversion is an excitonic circuit, with an exothermic pathway for excitons from the sensitizer to the annihilator. But it is important to consider the possibility that some excitons could also dissociate into free carriers, which could lead to triplet-charge annihilation (TCA) that results in the nonradiative loss of triplet excitons and a reduction in upconverted PL. We measure the magnetic field effect (MFE) of the upconverted PL for all devices to identify if there is evidence for TCA in our system, based on the fact that TTA and TCA have distinct MFE curves according to the model proposed by Merrifield et al. (Supporting Information).^[29,30] **Figure 3c** shows the MFE curves for the upconversion devices, indicating that a combination of TTA and TCA is at play. These data demonstrate that, in addition to back transfer and sensitizer aggregation, charge accumulation and consequent TCA is an additional loss pathway limiting the efficiency of TTA in rigid solid-state devices.^[31] This charge accumulation can be attributed to the alignment of highest occupied molecular orbital (HOMO) and lowest unoccupied molecular orbital (LUMO) at the heterojunction. **Figure S5a** suggests that it is preferable for electrons to transfer to the annihilator while leaving holes behind in the sensitizer. To test the significance of TCA in reducing upconversion efficiency, we fabricate a device based on the DMPPP-doped device to remove charge at the interface: indium tin oxide (ITO)/Di-[4-(N,N-ditolyl-amino)-phenyl]-cyclohexane (TAPC)/DMPPP-doped/Tris-[3-(3-pyridyl)mesityl]borane (3TPYMB)/LiF/Al. Upon

applying reverse bias, the upconverted PL is enhanced by 6.4% as shown in **Figure 3d**. Given that the contacted device is not well-optimized for efficient charge extraction (**Figure S5b**), this result indicates TCA is responsible for a minimum of 6.4% reduction in upconversion efficiency for the DMPPP-doped device.

Because of the relatively similar MFE magnitudes in **Figure 3c**, we assume the combination of ϕ_{TTA} and $(1 - \phi_{TCA})$ is the same for all devices, where ϕ_{TCA} is the TCA efficiency in the device. With this assumption, the enhancement in ϕ_{DET} relative to the Bilayer device for the Buffer, Triple-doped, and DMPPP-doped devices can be calculated using Equation (1), giving ~ 1.3 , ~ 14 , and ~ 7.2 , respectively.

The overall upconversion efficiencies and loss processes in each device are summarized in **Table 1**. We focus first on the Buffer device. Compared to the Bilayer device, it is notable that ϕ_{UC} for the Buffer device is enhanced by ~ 1.4 -fold, despite the reduced ϕ_{BT} improving the efficiency by only a factor of ~ 1.03 . This difference is due to improved triplet transfer efficiency, which is possibly surprising because the buffer material adds to the required diffusion length for triplet excitons to transfer to the annihilator. The increase in triplet transfer efficiency in the Buffer device can be attributed to the higher triplet energy in DMPPP than in MADN, which confines triplet excitons within MADN. In other words, the buffer material blocks both singlet and triplet back transfer from the annihilator to the sensitizer.

Despite its conceptual advantages, the Buffer device does not exhibit the highest overall efficiency. To maximize the benefit from the buffer layer, three further details should be considered. First, the thickness of the DMPPP layer should be optimized in order to overcome longer-range FRET from MADN:BDAVB_i to PtOEP while simultaneously allowing for efficient short-range triplet exciton diffusion to generate triplet excitons in the annihilator. Second, DMPPP may not be the best choice as buffer material for our system because the triplet energy of DMPPP lies slightly above that of

PtOEP, which could limit the triplet transfer efficiency from PtOEP to DMPPP because the process is partially endothermic. Third, observation of upconverted PL in a bilayer of PtOEP/DMPPP indicates additional triplet loss during diffusion within the buffer layer. This is considered as a loss pathway because the upconverted singlet excitons formed in the DMPPP buffer are likely quenched by PtOEP instead of transferring to MADN:BDAVBi for emission (**Figure S4c**). We summarize the criteria for choosing a buffer material for solid-state upconversion systems as follows: (1) The buffer's singlet state should be higher than that of the annihilator, (2) the triplet exciton energy as determined by its phosphorescence spectrum should lie entirely between that of the sensitizer and that of the annihilator, and (3) the singlet and higher-lying triplet energies should be greater than twice the lowest-lying triplet energy. Criteria (1) and (2) are needed to block annihilator-to-sensitizer back transfer while enabling efficient triplet sensitization of the annihilator. Criterion (3) is important so as to minimize parasitic upconversion in the buffer layer. Following these criteria, we speculate that the ideal buffer material would be an exothermic singlet fission molecule with triplet energy between that of the sensitizer and the annihilator. It is challenging to find a promising buffer material for green-to-blue upconversion systems due to the lack of singlet fission materials with triplet energy above 1.4 eV.^[32]

Contrary to the marginal improvement of ϕ_{UC} in the Buffer device as compared to the Bilayer device, significant enhancements are observed in the Triple-doped and DMPPP-doped devices, indicating that triplet transfer from PtOEP to MADN dominates the loss in our system. As expected, the Triple-doped device exhibits both the best ϕ_{DET} and the strongest back transfer. An extremely low concentration of PtOEP (< 0.1 vol.%) can potentially turn off back transfer,^[14] but it is challenging to achieve such low doping percentage using thermal evaporation because the rate deviation during deposition is close to the order of the target concentration. By increasing the average separation of PtOEP molecules while spatially separating the annihilator and the sensitizer, the DMPPP-doped

device provides an alternate way to reduce sensitizer aggregation while simultaneously limiting back transfer.

In addition to upconversion efficiency, the threshold excitation intensity at which the upconversion devices operate at their peak efficiencies is also an important factor for practical applications. The upconverted PL that results from TTA upconversion has a unique dependency on the excitation intensity that changes from quadratic to linear with increasing incident intensity, and the transition point represents the threshold intensity at which TTA reaches its peak efficiency (Supporting Information).^[33,34] **Figure 4** depicts the excitation intensity dependence of upconverted PL in our devices, with the threshold intensities determined as 1404 mW/cm², 704 mW/cm², 971 mW/cm², and 238 mW/cm² for the Bilayer, Buffer, Triple-doped, and DMPPP-doped devices, respectively. (For a detailed explanation of the fitting method used to determine these threshold intensities, and for a discussion of the deviation of the data from the fits, see Supporting Information and **Figure S6**.) Interestingly, despite the relatively small ϕ_{UC} improvement for the Buffer device compared to the Bilayer device, the threshold intensity is significantly decreased, likely as a result of reduced back transfer of triplet excitons. For the Triple-doped and DMPPP-doped devices (for which ϕ_{UC} is very high compared to the Bilayer device), the threshold intensity for the DMPPP-doped device is ~4 times lower than that of the Triple-doped device. This can be attributed to the higher sensitizer absorption and better triplet exciton confinement in the DMPPP-doped device.

Based on overall upconversion performance, the DMPPP-doped device demonstrates a superior ϕ_{UC} and a low threshold intensity. To our knowledge, this is the first demonstration of a completely dry-processed solid-state TTA upconversion system having comparable performance to solution-processed solid-state systems.^[13,14,23,35–38] Further improvements could be realized by choosing materials with longer triplet diffusion length as sensitizer, employing a buffer material that enables efficient triplet transfer and blocks back transfer without undergoing upconversion itself,

and selecting a host material for the sensitizer that has HOMO and LUMO levels that minimize charge accumulation at the sensitizer/annihilator interface.

In conclusion, we demonstrate strategies capable of addressing the two major losses affecting solid-state photon upconversion: back transfer and sensitizer aggregation. To minimize back transfer, keeping the sensitizer and the annihilator in separated layers is shown to be an effective approach, and introduction of a buffer layer where triplet exciton annihilation is energetically unfavorable could further enhance the device performance. To suppress sensitizer aggregation, a bilayer structure with the sensitizer doped into a host material is shown to reduce molecular aggregation while minimizing back transfer. Triplet-charge annihilation is identified as a third loss pathway. While not a dominant factor in our system, triplet-charge annihilation should be considered as an important loss pathway when choosing material systems for solid-state TTA upconversion. Following these techniques, we report a solid-state upconversion device with a reasonable ϕ_{UC} of 2.46% at a relatively low threshold intensity of 238 mW/cm². The strategies presented in this work for overcoming back transfer and sensitizer aggregation can be generalized to other TTA upconversion systems and provide a pathway to achieving high performance solid-state TTA upconversion devices.

Experimental Section

Sample Preparation: All materials were purchased from Luminescence Technology Corp. and used as received. Upconversion devices were fabricated through thermal evaporation on glass substrates in a vacuum chamber with a base pressure of $<10^{-6}$ torr. The device for reverse bias measurement was fabricated in the same chamber and the same vacuum level as all other samples, with the substrate being patterned indium tin oxide (ITO). The organic layers were deposited with a square mask, followed by the final metal layer where another patterned mask was applied to form 8 devices with

a size of 1 mm × 3 mm on one ITO substrate. Thin films for triplet phosphorescence measurements were prepared with a mixture of the following solutions: (1) 490 µL of poly(4-bromostyrene) (4-BrPS) in anisole (20 mg/mL); and (2) 200 µL of DMPPP or MADN in anisole (1 mg/mL). 100 µL of the mixed solution was dropcast onto a glass substrate, and the substrate was left on a hotplate at 65°C to dry and form thin films of 4-BrPS: 2 wt.% DMPPP and 4-BrPS: 2 wt.% MADN. Encapsulation was carried out for all the samples using UV-curable epoxy in a nitrogen-filled glovebox before transferring samples to an ambient environment for characterization.

Characterizations: All the measurement details and the necessary theories are described in Supporting Information.

Supporting Information

Supporting Information is available from the Wiley Online Library or from the author.

Acknowledgements

This work was supported by the U.S. Department of Energy, Office of Basic Energy Sciences (Award No. DE-FG02-07ER46474).

Received: ((will be filled in by the editorial staff))

Revised: ((will be filled in by the editorial staff))

Published online: ((will be filled in by the editorial staff))

References

- [1] R. R. Islangulov, D. V. Kozlov, F. N. Castellano, *Chem. Commun.* **2005**, 1, 3776.
- [2] S. Balushev, T. Miteva, V. Yakutkin, G. Nelles, A. Yasuda, G. Wegner, *Phys. Rev. Lett.* **2006**, 97, 143903.
- [3] J. Zhou, Q. Liu, W. Feng, Y. Sun, F. Li, *Chem. Rev.* **2015**, 115, 395.
- [4] B. Joarder, N. Yanai, N. Kimizuka, *J. Phys. Chem. Lett.* **2018**, 9, 4613.
- [5] T. N. Singh-Rachford, F. N. Castellano, *Coord. Chem. Rev.* **2010**, 254, 2560.
- [6] T. W. Schmidt, F. N. Castellano, *J. Phys. Chem. Lett.* **2014**, 5, 4062.
- [7] T. Ogawa, N. Yanai, A. Monguzzi, N. Kimizuka, *Sci. Rep.* **2015**, 5, 1.
- [8] C. Ye, J. Wang, X. Wang, P. Ding, Z. Liang, X. Tao, *Phys. Chem. Chem. Phys.* **2016**, 18, 3430.
- [9] X. Cao, B. Hu, P. Zhang, *J. Phys. Chem. Lett.* **2013**, 4, 2334.
- [10] R. S. Khnayzer, J. Blumhoff, J. A. Harrington, A. Haefele, F. Deng, F. N. Castellano, *Chem. Commun.* **2012**, 48, 209.
- [11] B. D. Ravetz, A. B. Pun, E. M. Churchill, D. N. Congreve, T. Rovis, L. M. Campos, *Nature* **2019**, 565, 343.
- [12] L. Huang, Y. Zhao, H. Zhang, K. Huang, J. Yang, G. Han, *Angew. Chemie Int. Ed.* **2017**, 56, 14400.
- [13] V. Gray, K. Moth-Poulsen, B. Albinsson, M. Abrahamsson, *Coord. Chem. Rev.* **2018**, 362, 54.
- [14] T. Ogawa, M. Hosoyamada, B. Yurash, T. Q. Nguyen, N. Yanai, N. Kimizuka, *J. Am. Chem. Soc.* **2018**, 140, 8788.

- [15] M. Wu, D. N. Congreve, M. W. B. Wilson, J. Jean, N. Geva, M. Welborn, T. Van Voorhis, V. Bulović, M. G. Bawendi, M. A. Baldo, *Nat. Photonics* **2016**, *10*, 31.
- [16] T. Trupke, M. A. Green, P. Würfel, *J. Appl. Phys.* **2002**, *92*, 4117.
- [17] F. L. Meng, J. J. Wu, E. F. Zhao, Y. Z. Zheng, M. L. Huang, L. M. Dai, X. Tao, J. F. Chen, *Nanoscale* **2017**, *9*, 18535.
- [18] L. Graf Von Reventlow, M. Bremer, B. Ebenhoch, M. Gerken, T. W. Schmidt, A. Colmann, *J. Mater. Chem. C* **2018**, *6*, 3845.
- [19] M. Häring, R. Pérez-Ruiz, A. J. Von Wangelin, D. D. Díaz, *Chem. Commun.* **2015**, *51*, 16848.
- [20] P. B. Merkel, J. P. Dinnocenzo, *J. Lumin.* **2009**, *129*, 303.
- [21] H. Fukagawa, T. Shimizu, N. Ohbe, S. Tokito, K. Tokumaru, H. Fujikake, *Org. Electron. physics, Mater. Appl.* **2012**, *13*, 1197.
- [22] R. Kim, S. Lee, K. H. Kim, Y. J. Lee, S. K. Kwon, J. J. Kim, Y. H. Kim, *Chem. Commun.* **2013**, *49*, 4664.
- [23] T. C. Wu, D. N. Congreve, M. A. Baldo, *Appl. Phys. Lett.* **2015**, *107*, 031103.
- [24] C. H. Chen, N. T. Tierce, M. kit Leung, T. L. Chiu, C. F. Lin, C. J. Bardeen, J. H. Lee, *Adv. Mater.* **2018**, *30*, 1804850.
- [25] P. Y. Chou, H. H. Chou, Y. H. Chen, T. H. Su, C. Y. Liao, H. W. Lin, W. C. Lin, H. Y. Yen, I. C. Chen, C. H. Cheng, *Chem. Commun.* **2014**, *50*, 6869.
- [26] T. Dienel, H. Proehl, T. Fritz, K. Leo, *J. Lumin.* **2004**, *110*, 253.
- [27] D. Davydova, A. De La Cadena, S. Demmler, J. Rothhardt, J. Limpert, T. Pascher, D. Akimov, B. Dietzek, *Chem. Phys.* **2016**, *464*, 69.

- [28] J. C. de Mello, H. F. Wittmann, R. H. Friend, *Adv. Mater.* **1997**, 230.
- [29] R. E. Merrifield, *J. Chem. Phys.* **1968**, 48, 4318.
- [30] R. E. Merrifield, P. Avakian, R. P. Groff, *Chem. Phys. Lett.* **1969**, 3, 386.
- [31] N. J. Thompson, E. Hontz, D. N. Congreve, M. E. Bahlke, S. Reineke, T. Van Voorhis, M. A. Baldo, *Adv. Mater.* **2014**, 26, 1366.
- [32] C. F. Perkinson, D. P. Tabor, M. Einzinger, D. Sheberla, H. Utzat, T.-A. Lin, D. N. Congreve, M. G. Bawendi, A. Aspuru-Guzik, M. A. Baldo, *J. Chem. Phys.* **2019**, 151, 121102.
- [33] D. Y. Kondakov, *J. Appl. Phys.* **2007**, 102, DOI 10.1063/1.2818362.
- [34] D. Y. Kondakov, T. D. Pawlik, T. K. Hatwar, J. P. Spindler, *J. Appl. Phys.* **2009**, 106, DOI 10.1063/1.3273407.
- [35] X. Jiang, X. Guo, J. Peng, D. Zhao, Y. Ma, *ACS Appl. Mater. Interfaces* **2016**, 8, 11441.
- [36] V. Jankus, E. W. Snedden, D. W. Bright, V. L. Whittle, J. A. G. Williams, A. Monkman, *Adv. Funct. Mater.* **2013**, 23, 384.
- [37] T. Ogawa, N. Yanai, H. Kouno, N. Kimizuka, *J. Photonics Energy* **2017**, 8, 022003.
- [38] L. Nienhaus, J. P. Correa-Baena, S. Wiegold, M. Einzinger, T. A. Lin, K. E. Shulenberger, N. D. Klein, M. Wu, V. Bulović, T. Buonassisi, M. A. Baldo, M. G. Bawendi, *ACS Energy Lett.* **2019**, 4, 888.

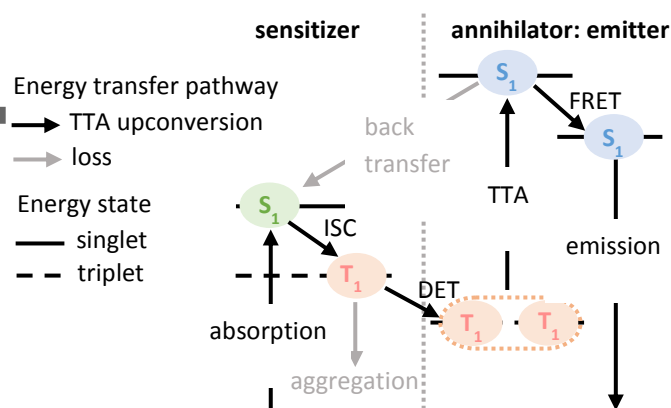


Figure 1. Schematic of a solid-state TTA upconversion system. ISC: intersystem crossing; DET: Dexter energy transfer; TTA: triplet-triplet annihilation; FRET: Förster energy transfer.

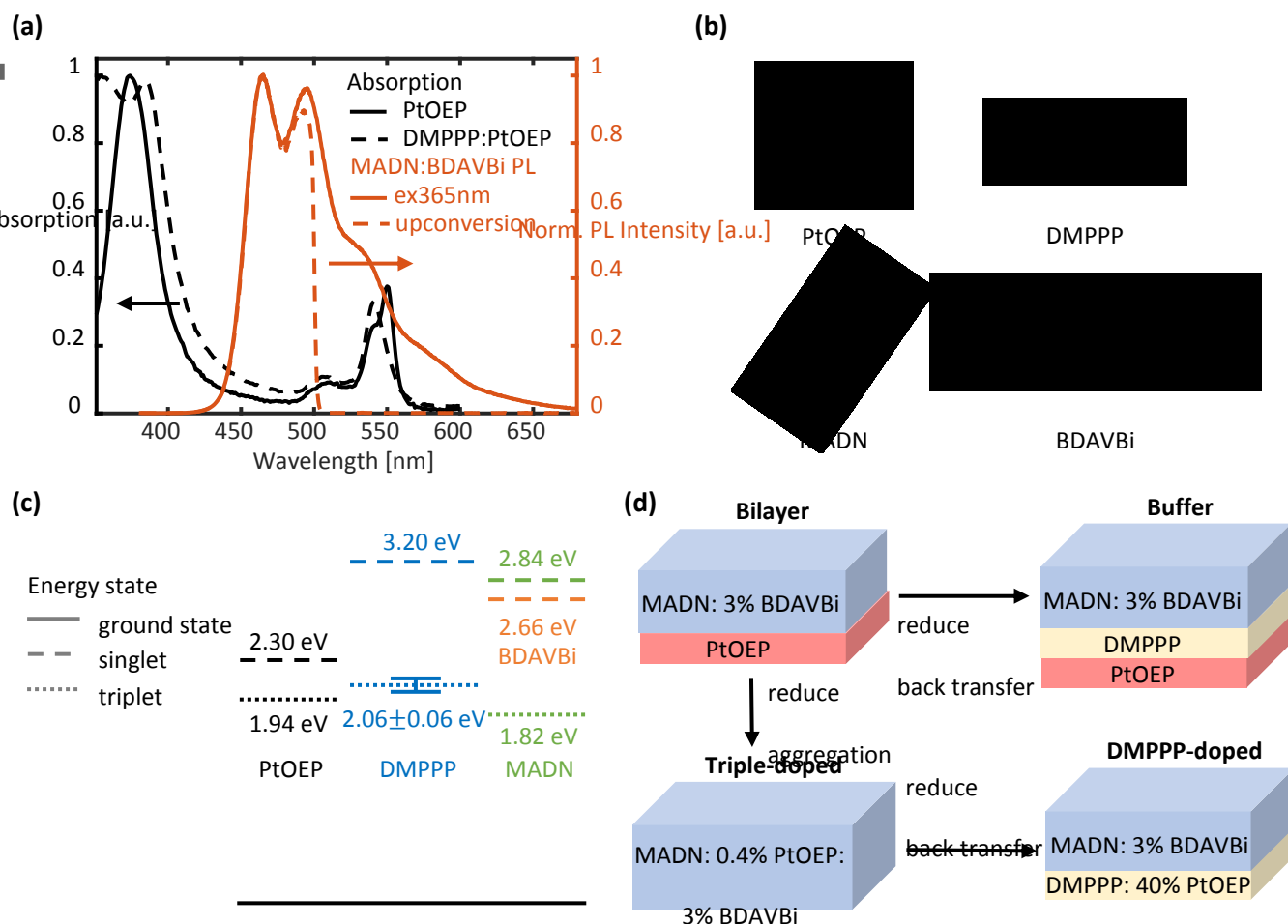


Figure 2. (a) Absorption spectra for PtOEP (2 nm) and DMPPP: 40 vol.% PtOEP (5 nm), and PL spectra for MADN: 3 vol.% BDAVBi (50 nm) at excitation wavelengths of 365 nm and 532 nm (upconversion). A 500 nm shortpass filter was applied in collecting the upconverted PL spectrum in order to minimize scattered laser signal. (b) Molecular structure and (c) energy diagram (not to scale) for the materials used in the devices. (d) Device structures (not to scale) and design concept for the four upconversion devices presented in this work.

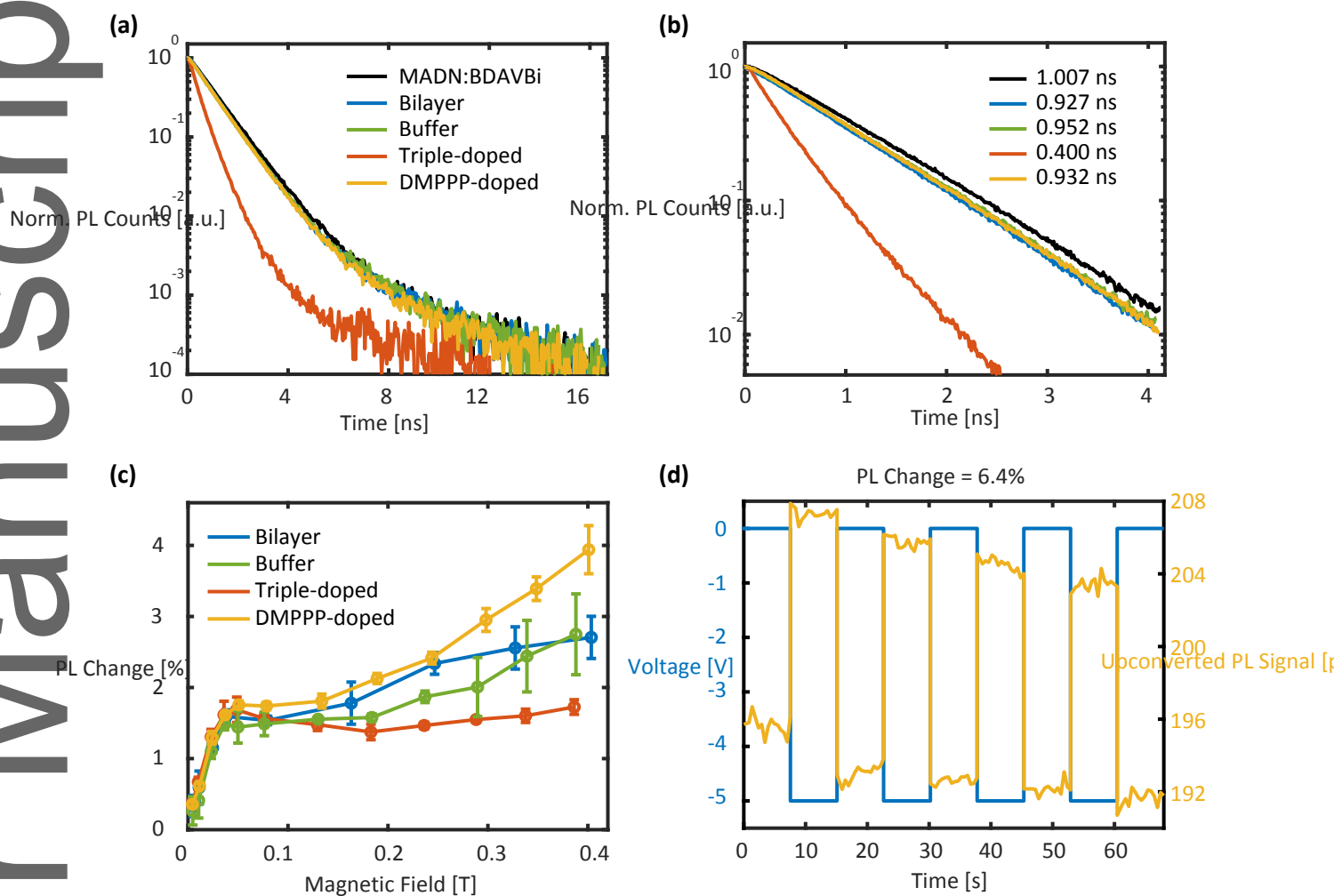


Figure 3. (a–b) Transient PL decay curves for MADN:BDAVBi film and the four upconversion devices at 372 nm excitation in 16 ns scale and 4 ns scale. **(c)** Magnetic field effect of upconverted PL for the four devices, with shapes indicating a combination of triplet-triplet annihilation and triplet-charge annihilation. **(d)** Enhancement in upconverted PL under reverse bias for the DMPPP-doped device, indicating that upconversion efficiency is reduced by at least 6.4% due to triplet-charge annihilation.

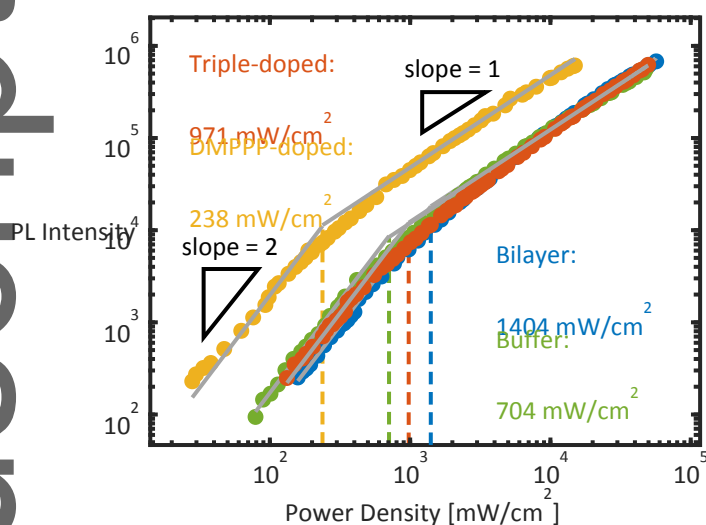
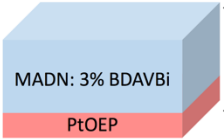
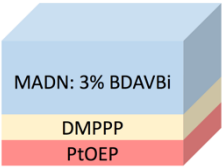
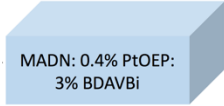
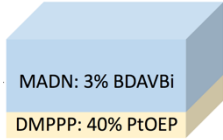


Figure 4. Intensity dependence of upconverted PL for the four devices at 532 nm excitation. A 500 nm shortpass filter is applied in collecting the upconverted PL to minimize scattered laser signal. The threshold intensities are determined by the transition point of quadratic-to-linear dependency. The DMPPP-doped device exhibits a ~6-fold reduction of threshold intensity compared to the Bilayer device. The fitting method is detailed in the Supporting Information, with upconversion data for each device reported individually in **Figure S6** for clarity.

Table 1. Summary of the device performance. *Abs*: absorption of the devices at 532 nm excitation; EQE: external quantum efficiency; ϕ_{UC} : upconversion efficiency, calculated from *Abs* and EQE through $\phi_{UC} = 2 \times \text{EQE} / \text{Abs}$; ϕ_{BT} : back-transfer efficiency, determined by the decay lifetimes in Figure 2b; ϕ_{DET} : efficiency of triplet transfer from the sensitizer to the annihilator, calculated with the assumption that the combination of triplet-triplet annihilation and triplet-charge annihilation has similar effect on upconversion efficiency for all devices.

	Bilayer	Buffer	Triple-doped	DMPPP-doped
				
<i>Abs</i> [%] ^{a)}	1.91±0.05	1.84±0.20	0.40±0.008 ^{b)}	1.95±0.04
EQE [%] ^{a)}	(3.2±0.49)×10 ⁻³	(4.3±0.23)×10 ⁻³	(4.1±0.16)×10 ⁻³	(24±0.63)×10 ⁻³
ϕ_{UC} [%]	0.34±0.06	0.47±0.08	2.05±0.12	2.46±0.12
ϕ_{BT} [%]	7.9	5.5	60.3	7.5
ϕ_{DET} [a.u.]	1	1.3	14	7.2

^{a)} Measured with integrating sphere; ^{b)} Determined by linear extrapolation

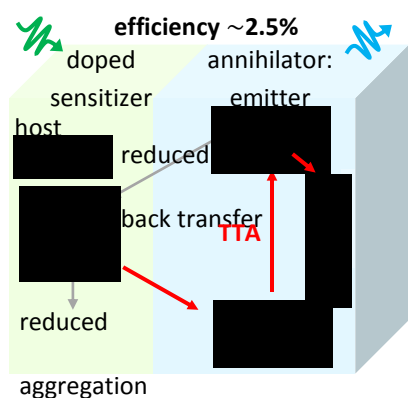
ToC Entry

Solid-state triplet-triplet annihilation-based photon upconversion systems are subject to losses from back transfer, molecular aggregation, and triplet-charge annihilation. Following the strategies provided to mitigate the losses, a dry-processed solid-state device having comparable upconversion efficiency and threshold intensity to solution-processed solid-state systems is developed, offering a route for high-performance upconversion devices compatible with applications sensitive to solvent damages.

Keyword solid-state photon upconversion

T.-A. Lin, C. F. Perkinson, and M. A. Baldo*

Strategies for High-Performance Solid-State Triplet-Triplet Annihilation Based Photon Upconversion



Copyright WILEY-VCH Verlag GmbH & Co. KGaA, 69469 Weinheim, Germany, 2018.